Computational and Experimental Investigation of Cavity Flowfields

O. Baysal*
Old Dominion University, Norfolk, Virginia
and
R.L. Stallings Jr.†
NASA Langley Research Center, Hampton, Virginia

Introduction

THE definition of cavity flowfields is important for application to cavities on contemporary and future aircraft and missile configurations capable of sustained supersonic flight speeds. A two-dimensional Navier-Stokes analysis utilizing an upwind relaxation scheme was conducted to compute the flows at the half-width symmetry plane of the cavity. The shocks were captured and turbulence was algebraically modeled. Experimental tests were also conducted in the Langley Unitary Plan Wind Tunnel (UPWT) for a box-cavity in a flat plate at zero angle of attack. The computational and experimental results were compared for flows with freestream Mach number, unit Reynolds number, and total temperature of 1.5, 2×10^6/ft, and 585°R, respectively, over cavities with length-to-depth ratios (L/D) of 6, 12, 16. The characteristics of open, closed, and transitional cavities were captured computationally as well as experimentally.

Contents

Computational Model

The conserved fluid properties, density, momentum, and total energy were contained in the vector U. Due to the significance of the streamwise gradients of the diffusion terms for the cavity flows, full Navier-Stokes equations had to be used. The integral form of Reynolds-averaged Navier-Stokes equations, which is solved computationally using a finite-volume method, is as follows:

$$\frac{\partial}{\partial t}\iint_{\Omega} U\,d\xi\,d\eta + \int_{\partial\Omega}\left[\left(F-\frac{R}{Re}\right)d\eta-\left(G-\frac{S}{Re}\right)d\xi\right]=0 \quad (1)$$

where Ω is a cell area with boundary $\partial\Omega$, ξ, and η are the generalized coordinates, t is time, F and G are fluxes containing the convective and pressure terms, R and S are fluxes containing the diffusive terms. Re is the ratio of freestream Reynolds number and Mach number. Air was assumed to be a perfect gas. The Sutherland formula and the Stokes hypothesis were used to determine molecular and bulk viscosities. The eddy viscosity was determined using the Baldwin-Lomax algebraic turbulence model.

The implicit finite-volume method of Thomas and Walters,[1] which employed upwind differencing for F and G, and central differencing for R and S, was used to solve Eq. (1). U was determined using Euler backward time integration and line-relaxation sweeps. The grids used contained approximately 9,000 cells. The cross-derivatives in the diffusive terms were excluded from the implicit formulation; they were computed explicitly at each time step. Global time stepping was used to ensure time accuracy.

Experimental Tests

The tests were conducted in the low Mach number test section of UPWT. The model consisted of a 41.9 in. long and 34.0 in. wide sting-mounted flat plate housing a cavity. The

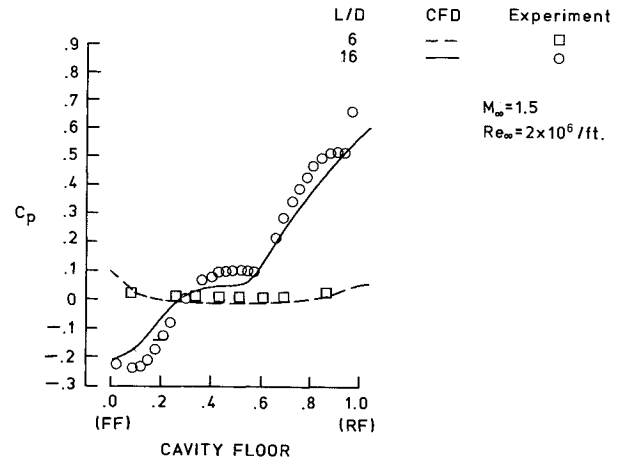

Fig. 1 Pressure coefficient (C_p) distributions over the cavity floor from the forward face (FF) to the rear face (RF).

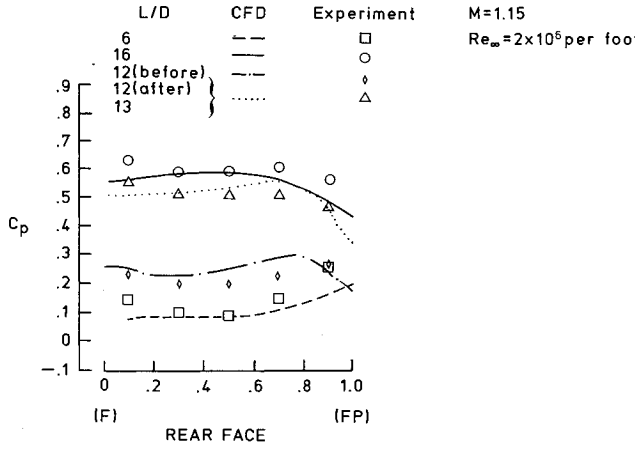

Fig. 2 Pressure coefficient (C_p) distributions over the cavity rear face from the floor (F) to the flat plate (FP): $M_\infty=1.5$, $Re_\infty=2\times10^6$/ft.

Presented as Paper 87-0114 at the AIAA 25th Aerospace Science Meeting, Reno, NV, Jan. 12–15, 1987; submitted Dec. 19, 1986; synoptic submitted June 1, 1987. Full paper available at AIAA Library, 555 W. 57th St., New York, NY 10019. Price: microfiche, $4.00; hard copy, $9.00. **Remittance must accompany order.**

*Assistant Professor, Mechanical Engineering and Mechanics Department. Member AIAA.

†Aerospace Engineer, Supersonic/Hypersonic Aerodynamics Branch. Member AIAA.

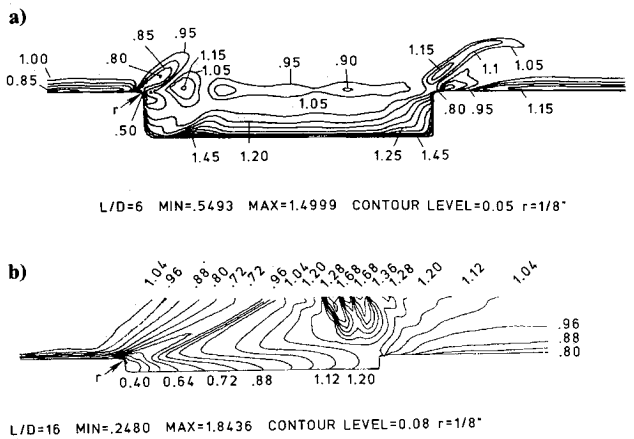

Fig. 3 Contours of computed instantaneous densities normalized with freestream density $M_\infty = 1.5$, $Re_\infty = 2 \times 10^6$/ft: a) $L/D = 6$ (open cavity), b) $L/D = 16$ (closed cavity).

forward face of the cavity was located 10.4 in. downstream of the flat plate leading edge where a boundary layer transition strip was applied. Cavity length (L) was remotely controlled by a sliding block assembly that formed the rear face of the cavity. The depth (D) and the width of the cavity were kept constant at 0.5 in. and 2.5 in., respectively. The model was instrumented with up to 84 static pressure orifices, depending on cavity length.

Results and Discussion

The results of this investigation provided time-averaged wall pressure data (Figs. 1 and 2) and flow visualization of the symmetry plane (Fig. 3) for cavities with L/D of 6, 12, and 16. The oncoming flow was turbulent with freestream Mach number, unit Reynolds number, and total temperature of 1.5, 2×10^6/ft, and 585°R, respectively. The measured boundary-layer thickness of the approaching flow at the front lip of the cavity was 0.2 in., which was matched exactly in the computations, with at least 20 grid cells within the boundary layer.

The experimental model had rectangular corners and measurements were averaged over periods of 1.0 s. The computational topology, however, had rounded corners to facilitate body-fitted grids, and the time-accurate calculations of wall pressures were averaged over periods of 0.1 s. Minor discrepancies between the computed results and experimental results may be attributed to these effects. Major contributors to the discrepancies, however, are believed to be the three-dimensional effects, such as the crossflow due to the sidewall of the cavity and the side flat plate, and the limited ability of the algebraic turbulence model to describe separated flows.

The pressure data and flow visualization obtained computationally and experimentally indicated flow separation on the forward face of the cavity and the formation of a highly vortical shear layer initiating at this face. The flowfield became dominated by regions of locally subsonic and supersonic flows. The shear layer bridged the $L/D = 6$ cavity separating the slow eddy inside the cavity from the freestream (Fig. 3a), hence it is called open cavity. The shear layer of $L/D = 16$ cavity, however, deflected inwards with an oscillating attachment point on the floor of the cavity, hence it is called closed cavity (Fig. 3b). An impingement-exit shock appeared to deflect the inward bound flow outwards and it became the cause of the separation on the cavity floor (Fig. 1). Two corner eddies appeared inside the cavity. For closed cavity, larger pressures were detected on the cavity rear face (Fig. 2) and smaller pressures were detected on the cavity front face than for open cavity flow. The Fourier time analyses were performed on the computed pressure histories at two floor locations of each cavity. The major harmonics of the flow oscillations were in the range of 2 to 9 kHz for the open cavity, and no significant harmonics were excited in the closed cavity.

A repetitive switching of the flow characteristics from open to closed cavity type was provided for approximately every 0.5 ms by the computations for the $L/D = 12$ cavity. In an attempt to show this "transitional" behavior, the computed wall pressure values before and after this switch are compared with the measurements of $L/D = 12$ and $L/D = 13$ cavities, respectively (Fig. 2). The L/D value of such a cavity is designated as the critical L/D. The experiments showed that the critical values of L/D obtained by increasing cavity length were greater than those obtained by decreasing cavity length, and that the magnitude of this hysteresis effect increased with increasing Mach number. The drag coefficients were determined to be 0.13, 0.27, and 0.88 for the cavities with L/D ratios of 6, 12, and 16, respectively.

Acknowledgment

This work was partially supported under NASA Grant NAG1-559.

Reference

[1]Thomas, J.L. and Walters, R.W., "Upwind Relaxation Algorithms for the Navier-Stokes Equations" AIAA Paper 85-1501, July 1985.